Chemical Engineering Journal 428 (2022) 131159

Contents lists available at ScienceDirect

Chemical Engineering Journal

journal homepage: www.elsevier.com/locate/cej

High-performance CdSe/CdS@ZnO quantum dots enabled by ZnO sol as surface ligands: A novel strategy for improved optical properties and stability

Lei Zhang [a], Hongyu Yang [b], Ying Tang [c], Wenbin Xiang [b], Chaonan Wang [a], Tian Xu [a], Xiaoyong Wang [c,*], Min Xiao [c,d], Jiayu Zhang [b,*]

[a] School of Science, Nantong University, Nantong 226019, China
[b] Advanced Photonics Center, School of Electronic Science & Engineering, Southeast University, Nanjing 210096, China
[c] National Laboratory of Solid State Microstructures, School of Physics, and Collaborative Innovation Center of Advanced Microstructures, Nanjing University, Nanjing 210093, China
[d] Department of Physics, University of Arkansas, Fayetteville, AR 72701, USA

ARTICLE INFO

Keywords:
Inorganic sol ligands
CdSe/CdS@ZnO QDs
Thermal stability
Optical gain
Vertical cavity surface-emitting laser

ABSTRACT

Colloidal semiconductor quantum dots (QDs) have attracted great attention in field of optoelectronic devices. However, the surface organic ligands of QDs involving in optical instability and limited passivation remain challenging, thus bringing additional difficulties in practical application. Here, the high-performance CdSe/CdS@ZnO QDs were successfully prepared by ZnO sol as surface ligands. Importantly, this kind of CdSe/CdS@ZnO QDs maintained the typical advantages of conventional QDs, such as superior monodispersity and long-term storage stability in solution. Because of the effective surface passivation provided by inorganic sol ligands and the deionization effect that electron transferring from surface state of QDs to ZnO acceptor, CdSe/CdS@ZnO QDs showed the remarkably enhanced photostability and biexciton lifetime, as well as further suppressed Auger process and PL blinking. Meanwhile, the CdSe/CdS@ZnO QDs demonstrated PL thermal stability much higher than that of pristine CdSe/CdS QDs under heating to 100 °C, which was efficiently improved 3 times that from ~20% to ~63% of their initial emission intensity. Moreover, a stable amplified spontaneous emission process was observed in CdSe/CdS@ZnO QDs film and still retained a lower ASE threshold (~28 μJ cm^{-2}). Finally, we successfully fabricated a high-performance vertical cavity surface-emitting laser based on CdSe/CdS@ZnO QDs, which presented spatially directional single-mode lasing output with an ultralow threshold of ~3.3 μJ cm^{-2}. We believe that this work could not only enrich the family of surface ligands passivated semiconductor QDs but also provide a novel strategy towards constructing stable and functionalized colloidal nanomaterials for all-inorganic optoelectronic devices.

1. Introduction

Colloidal semiconductor quantum dots (QDs) have emerged as promising materials owing to their superior optical properties in various potential applications, such as biomedical labeling, display backlights, lasers, and single-photon sources.[1–4] The surface organic ligands of QDs are necessary to ensure their optical performance and stability, which also provides a flexible choice for transforming their dispersion solvents environment, serving as a particular advantage for solution-processed fabrication of colloidal QD devices.[5–7] However, the inorganic–organic interface of QDs-ligand as a unique model system generally suffers from the insufficient passivation of undercoordinated surface atoms and particle aggregation, as a result of the partial desorption of organic ligands from QDs at different storage and application environment.[6,8,9] In this case, it easily resulted in an abundance of surface defects, which could act as surface trap states of excitons, and thus the deterioration in optical properties (such as low photoluminescence quantum yield (PL QY), PL blinking, and trap-induced Auger process).[8–12] Additionally, the long insulating ligands would extremely prevent charge injection and limit the charge-transport property of materials, which was detrimental for the improvement of emission efficiency and stability of QD light-emitting

* Corresponding authors.
E-mail addresses: wxiaoyong@nju.edu.cn (X. Wang), jyzhang@seu.edu.cn (J. Zhang).

https://doi.org/10.1016/j.cej.2021.131159
Received 17 April 2021; Received in revised form 29 June 2021; Accepted 1 July 2021
Available online 6 July 2021

diodes.[13,14] So far, the improvement of optical properties relevant to QDs surface still remains a long-term open question in colloidal quantum dots fields, which is one of the most crucial factors for the realization of high-performance QD-based photovoltaic and optoelectronic devices.

In recent years, many approaches were proposed to suppress surface defects and improve the optical performance and photostability of QDs, which were usually implemented by epitaxially growing the inorganic shells on the surface of QDs or optimizing surface passivation by polymers or oxides encapsulation.[9,15–20] Originally, to address these issues, Core/shell heterostructure QDs have been extensively researched. For example, CdSe/CdS, CdSe/alloy-shell, and lead-halide perovskites-based core/shell structure and so on, that could obviously suppress surface trap sites of core QDs, resulting in the enhanced photostability and radiative recombination efficiency as well as optical gain performance.[5,15,21–27] However, the PL fluctuation phenomenon (blinking property) of single core/shell QD was extremely sensitive to surface trap and shell thickness, showing random switching of emission intensity between brightness states and dark states, indicating that there is still more or less adverse effect that from the surface states for the optical properties of core/shell QDs.[5,28–30] Since PL blinking of the QDs at single dot level has not been well controlled, thus the local environmental effects on single QD exciton state and its mechanism have been studying.[30–32] On the other hand, colloidal QDs could be also encapsulated in barrier materials to passivate surface trap states and prevent further deterioration of optical properties, such as capping or embedded into polymers or oxides (PMMA, PVA, PVP, SiO_2, TiO_2, ZrO_2, etc.) to reduce the sensitivity of QDs to oxygen, moisture, and temperature.[16–20,33,34] Although the remarkable enhancement of photostability and PL QY could be achieved by passivation effect of polymers or oxides matrix, it should be noted that most of the reported QDs composite systems were in multiple-particle level with poor dispersity and low ensemble uniformity. This was not ideal for film formation by the conventional solution-processed process and quite difficult to achieve several important applications at the single-particle level. Besides, the thick silica layer or excess matrix materials would inevitably reduce the packing density of QDs in film, thus could largely low their gain performance and against their potential opportunities for laser devices.[35,36] To our knowledge, the choice of best methods for achieving high-quality colloidal semiconductor QDs that free from the impact of surface organic ligands is still very limited. Hence, the optimized reconstruction scheme for the surface of QDs while maintaining good monodispersity and excellent gain performance for promising optoelectronic application is needed further exploration from new perspectives.

In this work, we put forward an efficient strategy to construct high-quality CdSe/CdS@ZnO QDs with inorganic ZnO sol as surface ligands for the first time. ZnO is a kind of environmentally friendly semiconductor with wide bandgap and high electron mobility. First, the CdSe/CdS@ZnO QDs were successfully prepared by a facile all-solution process at room temperature, and then the effects of ZnO sol ligands on the optical performance of CdSe/CdS QDs have been systematically studied. The ZnO sol not only can be regarded as surface ligands to efficiently passivate surface defects of CdSe/CdS QDs but also as electron acceptors to suppress the charged state of QDs, thus showing the increased PL emission efficiency and biexciton gain performance, as well as suppressed PL blinking. Notably, the as-prepared CdSe/CdS@ZnO QDs still possess good dispersity at single particle level and the ultrahigh room temperature storage stability in chloroform solution. At the same time, the coverage of ZnO sol protects the inner QDs from unfavorable external environment, thus the CdSe/CdS@ZnO QDs exhibit remarkably improved optical stability against UV irradiation and thermal treatment in contrast to the pristine CdSe/CdS QDs. Besides, CdSe/CdS@ZnO QDs exhibits stable amplified spontaneous emission (ASE) process with a lower gain threshold of $\sim$ 28 μJ cm^{-2}, which was comparable to the close-packed pure QDs film. Finally, a vertical cavity surface-emitting laser was fabricated using CdSe/CdS@ZnO QDs as gain medium layer, which realized high-performance single-mode lasing emission with an ultralow threshold of $\sim$ 3.3 μJ cm^{-2} and good operation stability. As a result, the proposal of the concept of inorganic sol ligands should be essential for improving the optical performance of colloidal semiconductor nanomaterials and further constructing all-inorganic optoelectronic devices.

2. Results and discussion

2.1. Preparation of CdSe/CdS@ZnO QDs

In order to overcome the deficiencies of organic ligands and further improving optical performance and stability, novel CdSe/CdS@ZnO QDs structure was here constructed for the first time using ZnO sol as surface ligands by a feasible all-solution process. Primarily, CdSe/CdS core/shell QDs with 5 and 11 CdS monolayers (MLs) were synthesized following a previous method.[34] Then, the synthesized QDs were purified by N-butyl ether to remove excess organic ligands from the QD surface (see Supporting Information). Fig. 1**a** shows the schematic diagram of the modification process on the surface of CdSe/CdS QDs using ZnO sol. First, to improve the intermiscibility between the QDs and sol, the surface treatment for QDs was carried out by mixing QDs with ethanolamine (EA) in chloroform solvent under stirring for 24 h (see Experimental section). Subsequently, the QDs were precipitated after the treatment with EA, indicating the loss of original ligands from the QD surface. From the FTIR spectra of CdSe/CdS QDs before and after treatment with EA, the oleate (COO^-) stretching modes near 1560 and 1408 cm^{-1} arisen from oleic acid (OA) ligands are almost disappeared in QDs treated with EA (Fig. 1**b**).[37] Furthermore, the characteristic C–H stretching vibrations at 2800–3000 cm^{-1} becomes stronger in EA treated QDs, which derived from hydrocarbon chain portion in EA.[38,39] These results indicate that most long-chain OA ligands originally attached on the QD surface were replaced by short-chain EA. This is consistent with the study by Dai et al., in which ethylenediamine assist ligand exchange and phase transfer of oleophilic QDs by stripping of original ligands from QDs surface.[6] At the same time, the steric hindrance of CdSe/CdS QDs was reduced because of the shorten chain length of surface ligands, thus leading to the poor dispersity stability and appearing precipitation.[40] Next, colloidal ZnO sol was added dropwise into the modified CdSe/CdS QDs solution while shaking until the QDs precipitation was redispersed well and became a clear and transparent solution, demonstrating the successful reconstruction of surface ligands using ZnO sol (**Fig. S1**). Also, the typical peaks between 1400 and 1600 cm^{-1}, as well as a broad band centered on 3300 cm^{-1} of ZnO sol are appeared in FTIR spectra of CdSe/CdS@ZnO QDs, further confirming that the ZnO sol was successfully capped on CdSe/CdS QDs (Fig. 1**b**). Importantly, the larger steric hindrance effect from a dense sol cross-linking network could contribute the EA treated QDs stably redispersed in solution.[41,42] Finally, we obtained the CdSe/CdS@ZnO QDs with the ZnO sol as ligands. In addition, the result has revealed that CdSe/CdS@ZnO QDs sample could stably store in chloroform solution for longer than 5 years, showing excellent dispersity stability at room temperature (**Fig. S2**).

2.2. Structural and optical characterization

The morphology of ZnO sol and above QDs samples was characterized by TEM (Fig. 1**c-f**). The thick-shell CdSe/CdS QDs (11 MLs) shows a good monodispersity, and with an average particle size of $\sim$ 11.12 nm (Fig. 1**d**). The conservation of the QDs shape after the EA treatment is confirmed with the TEM image (Fig. 1**e**), where the QDs appear easily aggregated due to the replacement of long-chain ligands by short-chain EA, which was consistent with the observed poor dispersity in solution. The TEM image of CdSe/CdS@ZnO QDs demonstrates that the sol capped QDs can be redispersed well and retains excellent ensemble

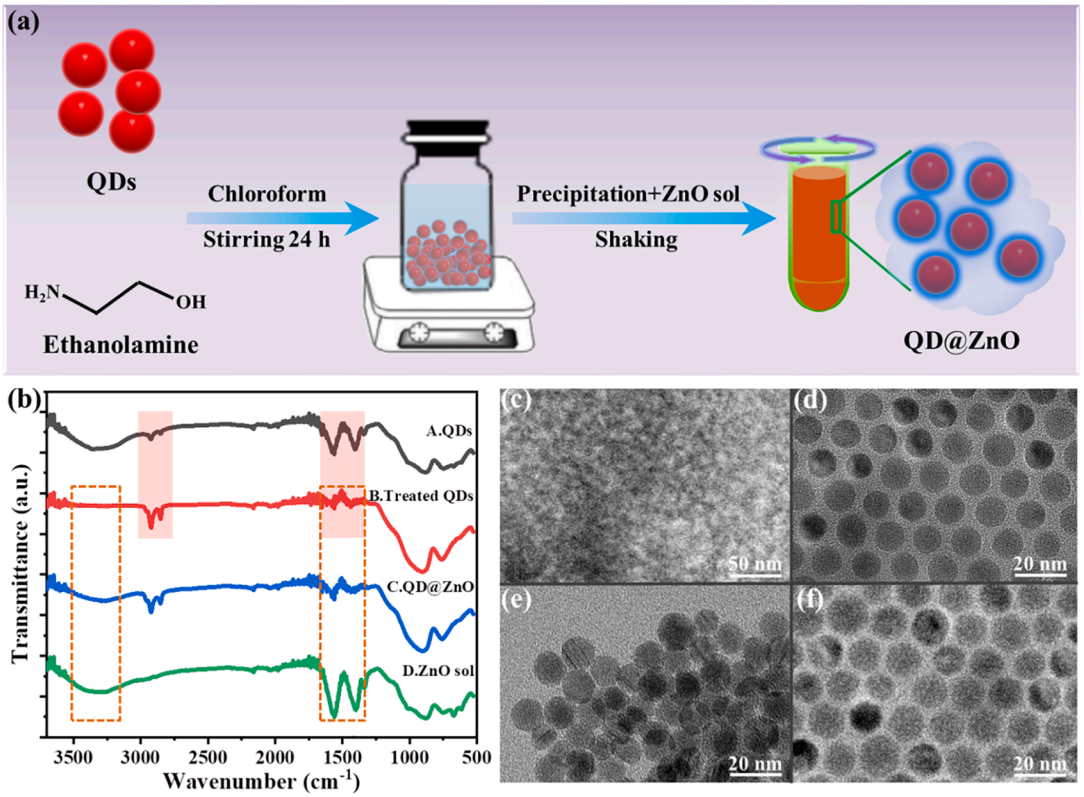

Fig. 1. (a) The schematic illustration for the preparation of CdSe/CdS@ZnO QDs. (b) Fourier transform infrared (FTIR) spectra of CdSe/CdS QDs (A), EA treated CdSe/CdS QDs (B), CdSe/CdS@ZnO QDs (C), and ZnO sol (D). (c-f) Transmission electron microscopy (TEM) images of ZnO sol, CdSe/CdS QDs, CdSe/CdS QDs treated with ethanolamine, and corresponding CdSe/CdS@ZnO QDs, respectively.

uniformity without particle aggregation (Fig. 1**f**), revealing a feature of fuzzy sol surface and boundary (Fig. 1**c and S3a**). The average diameter of CdSe/CdS@ZnO QDs was measured about ~ 12.24 nm, an average thickness of ZnO sol estimated to be ~ 0.56 nm by calculation based on the average size of CdSe/CdS QDs (**Fig. S3b**). The ZnO sol effectively protected CdSe/CdS@ZnO QDs from aggregations, thus improving the storage stability of QDs, which was similar to the function of traditional organic ligands. Therefore, CdSe/CdS@ZnO QDs could be applied in several important studies and applications demanding single particle level, which was an advantage that didn't have in most QDs composites. To intuitively verify the distribution of ZnO sol ligands, high-angle annular dark-field (HAADF) STEM elemental mapping measurement (Fig. 2**a-e**) was carried out, which confirmed that ZnO sol was successfully capping on CdSe/CdS QDs surface and there were very few unbound sol ligands on the blank area (Fig. 2**e**, red dashed area).

X-ray diffraction (XRD) characterization was employed to investigate the crystallographic structure of CdSe/CdS@ZnO QDs composite. Fig. 2**f** shows the XRD patterns of ZnO sol, CdSe/CdS QDs, and CdSe/CdS@ZnO QDs, respectively. The typical Wurtzite crystalline structure of ZnO was confirmed by five characteristic diffraction peaks.[43] The diffraction peaks of colloidal ZnO indexed to the (1 0 0), (1 0 1), and (1 1 0) planes could be observed in CdSe/CdS@ZnO QDs film. The other XRD peaks of ZnO were unconspicuous that maybe due to the superposition of peaks between CdSe/CdS and ZnO. Meanwhile, it is noteworthy that the diffraction peaks of ZnO in CdSe/CdS@ZnO QDs were weaker than those of pure ZnO film, because the surface of QDs was just capped by small amount of ZnO sol. Compared to the diffraction peaks in CdSe/CdS QDs and ZnO film, no noticeable shift of these peaks in CdSe/CdS@ZnO QDs was observed, indicating that the crystalline structure of CdSe/CdS QDs was not affected after ZnO sol modification and end up with a high-quality and stable QDs composite.

The optical properties of CdSe/CdS QDs before and after capping sol have also been monitored. Fig. 2**g** shows absorption and PL spectra of CdSe/CdS and CdSe/CdS@ZnO QDs. The absorption spectrum of CdSe/CdS@ZnO QDs almost showed no essential change as compared to that of the pristine CdSe/CdS QDs. The two absorption peaks could be still clearly observed following capping with ZnO sol and without distinct broadening. This result suggested that the original absorption property of CdSe/CdS@ZnO QDs was hardly affected by the introduction of ZnO sol, and still maintained uniform size distribution in ensemble level. Besides, the emission peaks of both samples from the PL spectrum were located at ~ 641 nm, with the similar full-width at half-maximum (FWHM) of ~ 27.8 nm and ~ 28.2 nm, respectively. It was no obvious red-shift and broadening of the emission peak in CdSe/CdS@ZnO QDs. This observation was typical of well-dispersed and colloidally stable QD samples, which was consistent with TEM measurement (Fig. 1**f**). As shown in the inset of Fig. 2**g**, the as-prepared CdSe/CdS@ZnO QDs solution exhibited bright red emission under UV irradiation. Besides, the detected maximum PL QY of CdSe/CdS@ZnO QDs could reach up to ~ 85%, which was higher than that of pristine CdSe/CdS QDs (~73%), which may be derived from the efficient surface passivation by ZnO sol ligands. These results are performed to demonstrate that there are no negative effects on the basic optical properties of QDs and their crystal structure that from the surface modification of ZnO sol ligands.

2.3. *Exciton dynamics and optical gain performance*

To research the passivation mechanism of ZnO sol for surface defects and their effects on exciton recombination dynamics of CdSe/CdS QDs, we measured the time-resolved PL decay dynamics process of the two samples. Fig. 3**a** presents the single-exciton PL decay traces of thick-shell CdSe/CdS QDs and corresponding CdSe/CdS@ZnO QDs, respectively. The PL decay traces could be well fitted with a biexponential decay function in the relaxation range longer than 400 ns. The fitting

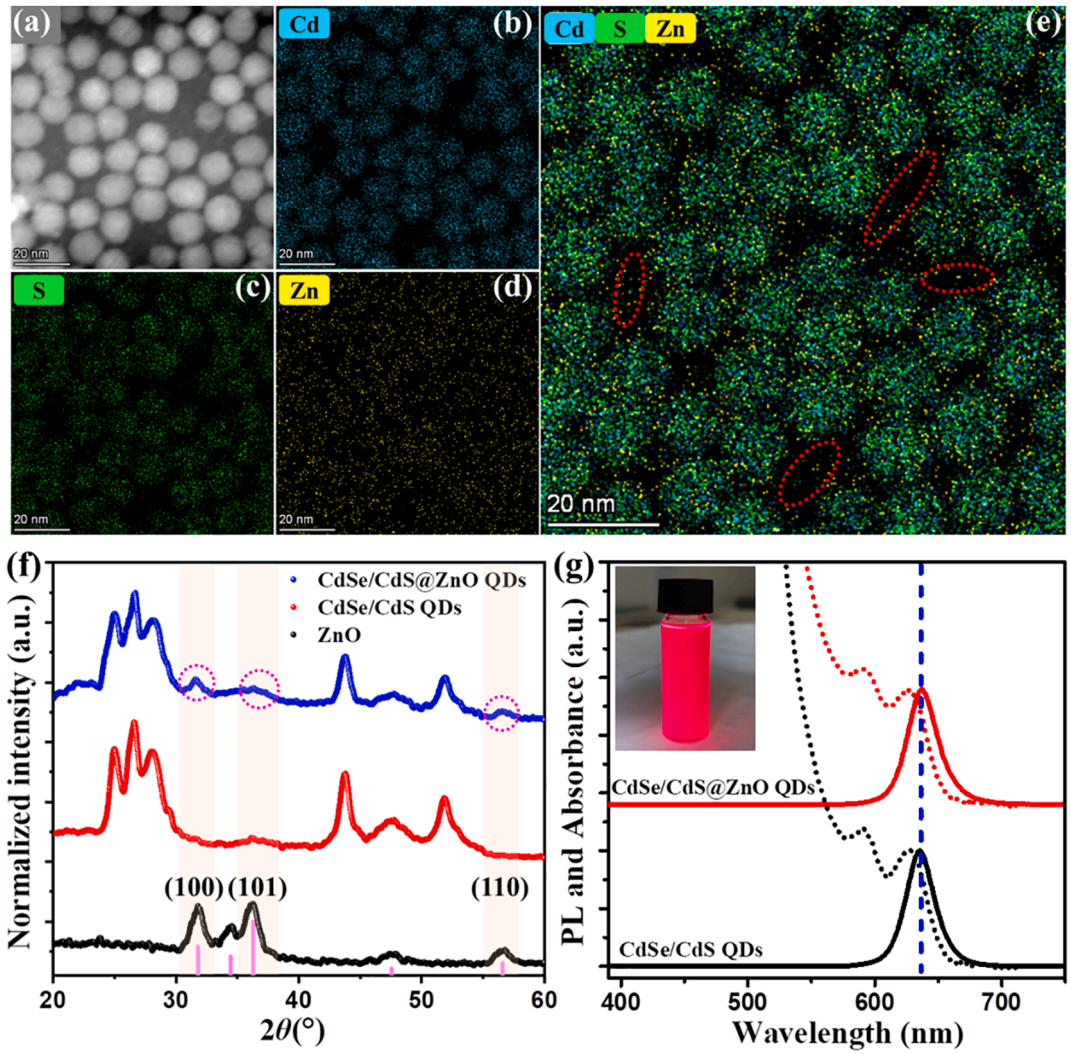

Fig. 2. (a) HAADF STEM image of CdSe/CdS@ZnO QDs. (b-e) Elemental mapping images showing the elemental distribution of CdSe/CdS@ZnO QDs. (f) XRD patterns of ZnO sol, CdSe/CdS QDs, and CdSe/CdS@ZnO QDs, the vertical solid line is standard XRD pattern of ZnO (pink) bulk crystal. (g) UV–vis absorption and PL spectra of thick-shell CdSe/CdS QDs (black line) and CdSe/CdS@ZnO QDs (red line). The spectra of CdSe/CdS@ZnO QDs are vertically shifted for clarity; the inset shows the photograph of CdSe/CdS@ZnO QDs solution under UV light irradiation. (For interpretation of the references to colour in this figure legend, the reader is referred to the web version of this article.)

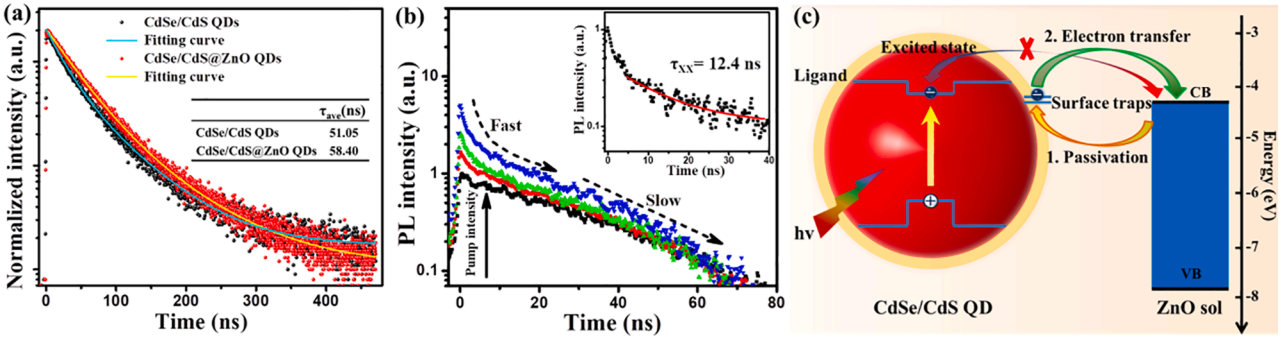

Fig. 3. (a) Single-exciton PL decay traces of thick-shell CdSe/CdS QDs (black) and CdSe/CdS@ZnO QDs (red); solid lines are fitted curves using biexponential function. (b) Time-resolved PL decay spectra of thick-shell CdSe/CdS@ZnO QDs pumped at 400 nm with increasing pump intensities; the insert shows that the biexciton lifetime (τ_{xx}) of CdSe/CdS@ZnO QDs is ~ 12.4 ns, extracted by the subtraction procedure. (c) Schematic diagram of the role of ZnO sol ligands towards CdSe/CdS QDs. (For interpretation of the references to colour in this figure legend, the reader is referred to the web version of this article.)

parameters are summarized in **Table S1** (See Supporting Information). As shown in insert of Fig. 3**a**, the average PL lifetime (τ_{ave}) increases from 51.05 ns for CdSe/CdS QDs to 58.40 ns for CdSe/CdS@ZnO QDs. The major difference in optical properties between the two samples is the ratio of the two decay components. According to the study of surface-related emission in QDs, the short-lived PL lifetime (τ_1) is

attributed to the radiative recombination of excitons insides in QDs, while the long-lived PL lifetime (τ_2) is related to the surface band-edge trap state assisted exciton recombination process.[10,44] With the capping of ZnO sol, the fraction of radiative recombination lifetime τ_1 increased from 64.17% to 80.60%, which were upto ~ 39.76 ns. Meanwhile, the trap-state emission lifetime τ_2 was reduced from a ratio of 35.83% to 19.40%. In particular, the changing trend of proportion of τ_1 and τ_2 in ZnO sol capped CdSe/CdS QDs indicates greatly improved radiative recombination efficiency and the reduction of nonradiative decay channels, because of the fact that the increased radiative recombination lifetime is a crucial factor that associated with the passivation of surface trap sites in semiconductor nanomaterials.[11,45] From these results and discussion, we could speculate that fewer defects and higher exciton radiative efficiency in CdSe/CdS@ZnO QDs. Therefore, the result demonstrates the efficient passivation effect provided by colloidal ZnO sol ligands for surface defects of CdSe/CdS QDs and consistent with the above PL QY analysis, which was similar to other QDs or perovskite system.[17,33,46]

In addition, we explored more insights into the biexciton recombination dynamics process of CdSe/CdS@ZnO QDs. The pump-dependent time-resolved PL decay spectra of CdSe/CdS@ZnO QDs were measured using a streak camera system (Fig. 3**b**). The biexciton lifetime τ_{xx} ~ 12.4 ns of CdSe/CdS@ZnO QDs is extracted from above PL decay traces by a subtraction procedure, as shown in insert of Fig. 3**b**.[47] The biexciton lifetime of CdSe/CdS@ZnO QDs is longer than that of CdSe/CdS QDs (~10 ns), indicating the enhanced biexciton gain performance.[27,34] Furthermore, we could estimate the biexciton Auger lifetime (τ_{2A}) of CdSe/CdS@ZnO QDs, which was to be of ~ 130 ns (See Supporting Information). Their τ_{2A} value reveals a further reduction of Auger decay rates compared to those of CdSe/CdS QDs.[34] Therefore, the extended biexciton Auger lifetime implies that the partial contribution for nonradiative Auger process that from the charged states at surface defects could be more effectively suppressed in this ZnO sol passivated CdSe/CdS QDs, thus further promoting the optical performance of thick-shell QDs as a superior gain medium.

Apart from the passivation effect of ZnO sol presenting in above experiment, another possible function of ZnO for improving optical performance of CdSe/CdS QDs is that it might act as electron acceptor. Hence, we here put forward a working mechanism of the ZnO sol in CdSe/CdS@ZnO QDs, the schematic illustration is as shown in Fig. 3**c**. In this model, thick CdS shells (11 MLs) could effectively prevent the photogenerated electrons insides CdSe/CdS QDs injecting into ZnO sol, which has been proved that it was nearly no electron transfer between QDs with shell thickness larger than 1.8 nm (~6 MLs) and ZnO nanoparticle.[48] Actually, the enhanced quantum efficiency and longer lifetime could also exclude the possibility of exciton transfer from the inner CdSe/CdS QDs to ZnO sol, even though with the appropriate conduction band energy level.[11,48] At the same time, the ZnO could not be excited and then generate excitons under the 400 nm pump conditions, because of their exciton absorption peak at ~ 307 nm (**Fig. S4**), thus proving the impossibility of carriers or energy transfer from ZnO to CdSe/CdS QD for enhancing optical performance of QDs. Besides, according to the previous relevant reports, the electron energy levels of shallow trap states on the surface of CdSe QDs are suggested near the band edge of emission state.[11,49,50] On these bases, the small conduction band offset between surface trap states and ZnO sol could facilitate the efficient transfer of trapped electron at the surface trap level of CdSe/CdS QDs into ZnO sol (Fig. 3**c**), which would remove the extra electron around the photoionized QDs. In this system, ZnO sol could be regarded as the synergistic role of electron acceptors and passivating ligands, thereby contributing to reduce the probability of charged state of QDs and maintain an electrically neutral local environment, and finally improve their PL efficiency. In principle, the deionized QDs are expected to recover bright states (neutral states) from the dark states (charged states), thus suppressing PL blinking behavior and the trap-induced nonradiative Auger losses as well as enhancing the radiative recombination efficiency.[9,28,32] Therefore, ZnO sol can not only passivate the QDs surface trap sites, but also possibly as electron acceptors further to avoid the effect of surface charged states on optical properties of QDs.

In order to confirm the above proposed model of ZnO sol as surface electron acceptor, the dynamic photophysical property of a single QD associated with surface states was measured. Particularly, we aimed to highlight the effect of sol ligands on the optical properties of QDs, whereas the thicker CdS shells could effectively suppress PL blinking of QDs,[21,28,34] thus medium-shell CdSe/CdS QDs (5 MLs) was selected as the sample for this study. Fig. 4**a,b** show the representative PL intensity trajectory as a function of time for single medium-shell CdSe/CdS QD and corresponding CdSe/CdS@ZnO QD, respectively.

As shown in Fig. 4**a**, the typical off period was observed in medium-shell CdSe/CdS QD with a long duration of ~ 40 s, which was usually thought to originate from the charged states inside or at the surface traps of a QD.[28] The counts of off fraction were upto ~ 12.8% and closed to the background level. In general, PL blinking behavior is the random switching between a bright state (on state) and dark state (off state) driven by charge transfer, accompanied by a charging and discharging process in QD.[9] For medium-shell CdSe/CdS@ZnO QD (Fig. 4**b**), the featured time-dependent PL intensity trajectory was almost always in the on state, which was consistent with an enhancement of the exciton radiative recombination. Meanwhile, the long off period was significantly suppressed and substantially far above the background level, and the off fraction was decreased lower than ~ 0.05%, indicating the charged medium-shell QD was deionized and tended to stabilize in a neutral state.[28,32] The effectively suppressed PL blinking in medium-shell CdSe/CdS@ZnO QD further indicates that ZnO sol not only acted as passivating ligands to protect CdSe/CdS QDs against surface states, but also may be as efficient electron acceptors that help to create and keep a stable electric neutrality environment around QDs. This point is also supported by the suppression of Auger process in CdSe/CdS@ZnO QDs as analyzed above, which could partially originate from the deionization effect for the photocharged sites on CdSe/CdS QDs by ZnO ligands. It is worth mentioning that the highly emissive bright state from the suppression of dark state at both single-dot and ensemble levels has been recently demonstrated in photoionized CdSe/CdS QDs via deionization of oxygen.[32] Consequently, the dual roles of surface passivation and electron acceptor provided by ZnO sol obtained higher PL QY, longer excitons lifetime, as well as suppressed PL blinking in these sol capped-QDs. Besides, the improved optical properties of QDs may also partially derive from the potential passivation of Zn^{2+} for surface localized electrons.

To further evaluate the photostability of the medium-shell CdSe/CdS@ZnO QDs, we performed a time-dependent emission intensity measurement of QDs solution under continuous 365 nm UV light irradiation. Fig. 4**c** shows the time revolution of PL intensity for medium-shell CdSe/CdS and CdSe/CdS@ZnO QDs under UV irradiation. During the first 2 h of irradiation, the enhanced emissions were observed for both QDs samples. The PL enhancement was commonly attributed to the surface rearrangement of ligands or photocatalytic annealing repair of surface defects.[51,52] Upon further UV irradiation (greater than2h), the emission intensity was decreased for both pristine and sol-capped CdSe/CdS QDs, but the decreasing tendency was more dominant in the case of CdSe/CdS QDs when directly exposed to solution compared to ZnO sol encapsulated QDs. After 17 h, the remnant PL intensity of CdSe/CdS QDs was reduced to ~ 21% of initial intensity. In contrast, the CdSe/CdS@ZnO QDs could finally maintain near ~ 90% of the original emission intensity following long duration of UV irradiation. As a result, the measured results suggested that the ZnO sol-passivated CdSe/CdS QDs are more photostable than naked CdSe/CdS QDs because of the efficient protection created by sol ligands. Besides for the surface protection effect of ZnO sol, another possible reason responsible for the improved stability of CdSe/CdS@ZnO QDs is the crucial surface treatment for QDs through EA. EA is a kind of short chain ligand modifying

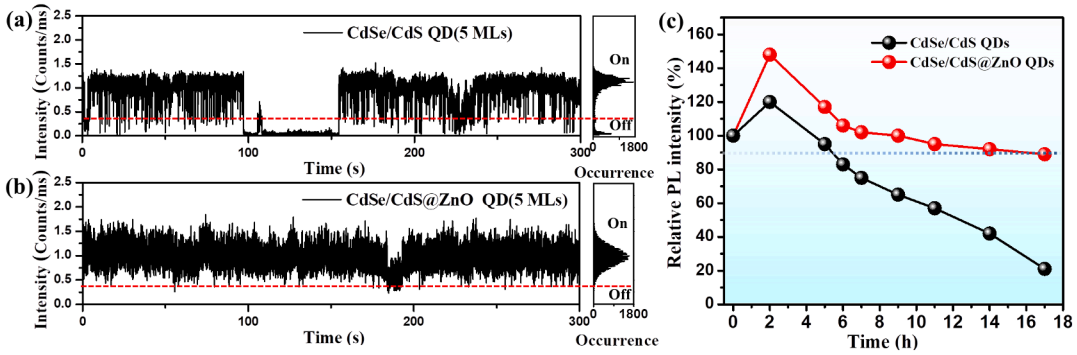

Fig. 4. The typical PL intensity trace as a function of time (binning time, 10 ms) for a single medium-shell (a) CdSe/CdS QD (5 MLs) and corresponding (b) CdSe/CdS@ZnO QD; the inset shows a histogram for the intensity distribution. (c) Time revolution of normalized PL intensity for the medium-shell CdSe/CdS and CdSe/CdS@ZnO QDs solution under UV light irradiation.

on the surface of these QDs, which could more enough passivate the surface trap sites with enhanced emission intensity (Fig. S5). Thus, the photostability under UV irradiation are further enhanced in these CdSe/CdS@ZnO QDs.

2.4. Optical thermal stability

Long-term environmental stability is one of the key factors for the application of QDs in display and light emitting devices, while optical thermal stability of luminescent materials is often severely tested in practical applications. Herein, both thick-shell CdSe/CdS and CdSe/CdS@ZnO QDs films were heated to 100 °C for the evaluation of their optical thermal stability. As shown in Fig. 5**a**, the PL intensity of CdSe/CdS QDs film was drastically decreased to below 50% during the first 20 min of heating. After 100 min thermal treatment, the relative PL intensity of CdSe/CdS QDs film gradually decreased to ~ 20% of initial intensity. Meanwhile, the decrease of PL intensity in CdSe/CdS QDs film was accompanied by a notable red shift (~2 nm) and gradual broadening (~2 nm) of emission peak after continuous thermal treatment (Fig. 5**a**, Fig. S6). This was mainly because heating induces the falling off of surface ligands, which made more surface defects exposure and the aggregation of CdSe/CdS QDs, resulting in the observed serious PL thermal quenching, emission redshift, and spectral broadening.[53,54]

In contrast, the emission intensity of the CdSe/CdS@ZnO QDs film was slowly decreased and finally maintained ~ 63% of their initial PL intensity after thermal treatment of 100 min (Fig. 5**b**), which was much more robust behavior than that found for CdSe/CdS QDs. Particularly, it is clear that no obvious emission shift and broadening were observed from the PL spectra of CdSe/CdS@ZnO QDs film following same thermal treatment (Fig. 5**b**, Fig. S6). Importantly, the FWHM (~28.4 nm) of emission spectra from CdSe/CdS@ZnO QDs film closed to that in CdSe/CdS@ZnO solution (Fig. S6), suggesting the ZnO sol ligands effectively protected the optical properties of CdSe/CdS QDs from the interactions among QDs in film. It should be noted that the compact and smoothed CdSe/CdS@ZnO QDs film was here prepared by a spin-coating and high-temperature annealing (300 °C) combined process, which wouldn't quench PL of ZnO sol capped QDs film (Fig. S7**a,b**). Accordingly, the external sol ligands could be the effective barrier between the QD materials and the ambience, because of the improvement of passivation effect during the crystallization period after annealing.[20,55] So, the inorganic sol ligands in CdSe/CdS@ZnO QDs film were more stable and without any volatilization under thermal treatment at 100 °C, thus exhibiting a much higher optical thermal stability than CdSe/CdS QDs and no obvious spectra changes (shift or broadening). Therefore, the ZnO sol ligands could provide the efficient protection to the inner CdSe/CdS QDs against optical properties degeneration under higher temperature environment.

2.5. Amplified spontaneous emission properties

Conventional QDs composites are usually encapsulated or embedded into polymer or oxide matrix to improve their stability and light-emission performance. However, these composite QDs films easily suffer from the reduced packing density of QDs due to the excess matrix materials, thus reducing their optical gain performance. So, we here plan to evaluate the effect of ZnO sol on the gain performance of CdSe/CdS@ZnO QDs film (volume fraction of ~ 52.3%) by ASE measurement. Fig. 6**a** shows the emission spectra of thick-shell CdSe/CdS@ZnO QDs

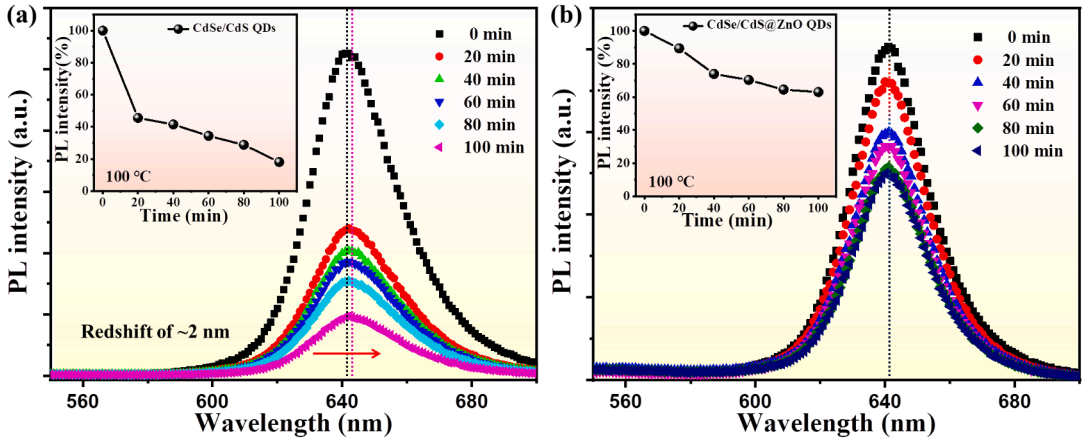

Fig. 5. Photostability of (a) thick-shell CdSe/CdS QDs film and corresponding (b) CdSe/CdS@ZnO QDs film under heating to 100 °C; the insert shows the emission intensity as a function of thermal treatment time.

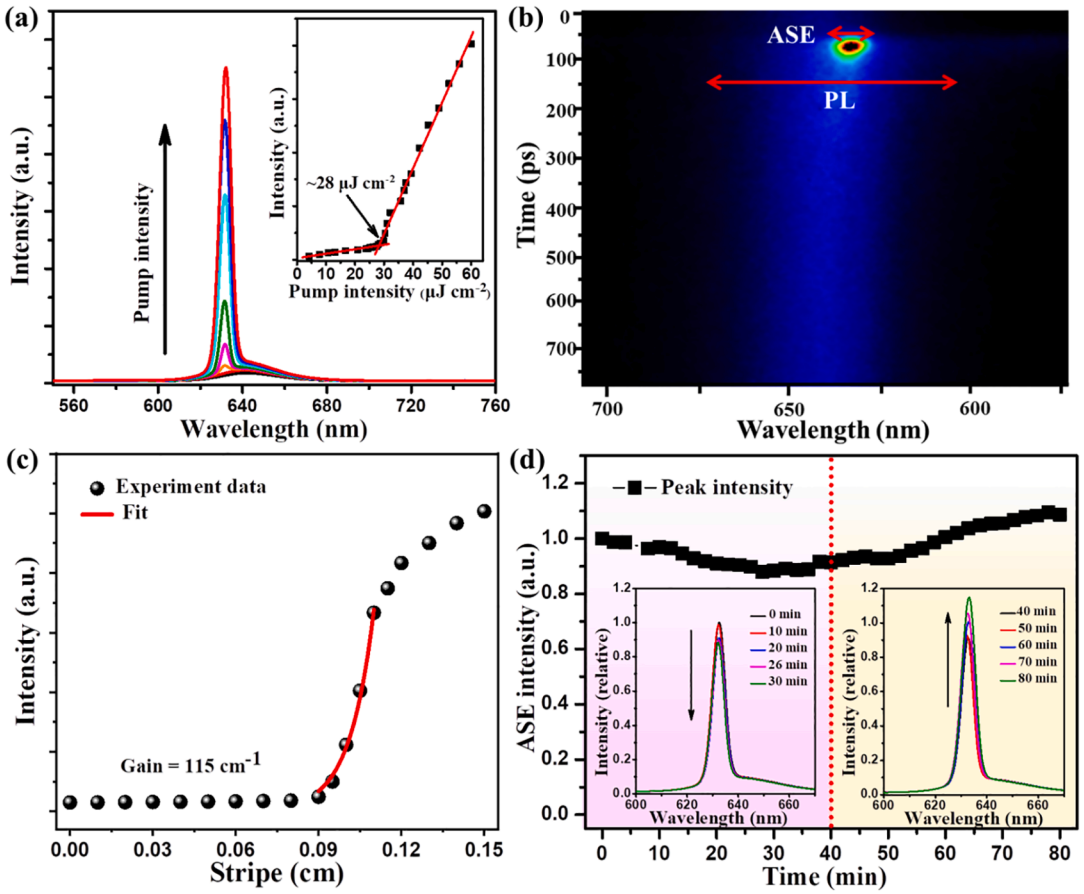

Fig. 6. (a) Pump-intensity dependence of the light emission from thick-shell CdSe/CdS@ZnO QDs film under femtosecond laser excitation at 400 nm; the inset shows their dependence of the output intensity as a function of pump intensity. (b) Time-resolved emission spectrogram of thick-shell CdSe/CdS@ZnO QDs film at a pump intensity of ~ 42 μJ cm^{-2}. (c) The variable stripe length (VSL) measurement of CdSe/CdS@ZnO QDs film. (d) Plot of ASE intensity of CdSe/CdS@ZnO QDs film measured under continuous pulsed femtosecond laser excitation; the inset shows the ASE spectra at the different excitation time.

film with increasing pump intensities under stripe femtosecond-pulsed excitation (**Fig. S7c**). As the increasing pump intensity, the emission spectra from the QDs film edge exhibited an obvious transition from spontaneous emission to ASE, along with the feature of spectral narrowing. The ASE threshold of CdSe/CdS@ZnO QDs was found to be as low as ~ 28 μJ cm^{-2}, which was comparable to the previously reported value for pure QDs film (~27 μJ cm^{-2}).[27] The gain threshold wasn't obviously decreased in CdSe/CdS@ZnO QDs even though the sol further passivated surface defects and self-enhanced biexciton gain, which might result from the reduced QD packing density in film after capping ZnO sol.[34] The peak wavelength of ASE spectra was detected at 632 nm with a narrow FWHM of ~ 6.7 nm (**Fig. S8**), which was narrower than that conventional QDs film (~8–9 nm). The narrow emission peak could be relevant to the better confined mode in high refractive index CdSe/CdS@ZnO QDs film and the process of sufficient internal reflection.[20,43]

Fig. 6**b** shows the time-resolved emission spectrogram of CdSe/CdS@ZnO QDs film as the pump intensity above ASE threshold, which includes PL and ASE two parts. The extracted emission spectra from time-resolved spectrogram of CdSe/CdS@ZnO QDs were shown in **Fig. S9a**. The obvious blueshift of ASE with respect to the PL was observed due to a repulsive exciton–exciton interaction in the thick-shell QDs.[56] The transient emission spectrum with long delay time (100–2000 ps) was dominated by single-exciton PL emission process, and the ASE only takes place within the initial 100 ps. At the same time, the evolution of their emission decay dynamics was also monitored at different pump intensity (**Fig. S9b**). The fast ASE lifetime could be finally reduced to ~ 20 ps, indicating an efficient ASE process.[27]

Besides, the effective modal gain of CdSe/CdS@ZnO QDs film was measured by the VSL method at the ASE peak (Fig. 6**c**).[36] The high gain coefficient was upto ~ 115 cm^{-1}, which was higher than the conventional semiconductor QDs-polymer film.[34]

Furthermore, the ASE stability of CdSe/CdS@ZnO QDs film was studied under pulsed femtosecond laser excitation. Fig. 6**d** shows the emission intensity of CdSe/CdS@ZnO QDs film at ASE peak as a function of excitation time. The representative emission spectra at different excitation times are shown in insert of Fig. 6**d**. In initial 40 min, the ASE intensity was slowly decreased to ~ 88% of primal intensity, which might be associated with the Auger ionization that occurred under multiexciton conditions.[20,57] Contrary to the previous situation, the slightly enhanced emission process was observed in the next 40–80 min, which was a ~ 1.1 time stronger than the initial intensity. The final emission performance tended to stay stabilization after 80 min of pump pulse excitation. The enhanced emission intensity maybe result from the removal of interfacial potential barrier in the valence band in such thick-shell QDs by femtosecond laser annealing, which could improve the relaxation efficiency of holes from the shell to the core.[58] The removed hole barrier could be also proved by the emission properties from the second (1P) quantization states (peaked at ~ 577 nm) of QDs, revealing the gradually enhanced recombination efficiency of higher-order excitons with laser annealing time (**Fig. S10**). Therefore, the outstanding ASE stability under intense laser excitation is encouraging for the prospective applications of CdSe/CdS@ZnO QDs in laser device.

2.6. Microlaser application based on CdSe/CdS@ZnO QDs

Finally, we make a meaningful exploration for the potential utilization value of CdSe/CdS@ZnO QDs as gain medium in microlaser. Fig. 7**a** presents the schematic configuration of laser device, which consists of a thick-shell CdSe/CdS@ZnO QDs layer and two high-reflectivity distributed Bragg reflector (DBR) mirrors. The corresponding cross-sectional scanning electron microscopy (SEM) image of the QD-VCSEL device was shown in **Fig. S11a**. Among, the whole microcavity reflectivity at emission peak was upto ~ 97% (**Fig. S11b**), and the photograph of the final device was shown in **Fig. S11c**. Fig. 7**b** displays the photograph of pump-intensity-dependent lasing operation of QD-VCSEL device, which realized the spatially directional lasing emission accompanied by a gradually bright and well-defined red spot as the increase of pump intensity. Fig. 7**c** shows the emission spectra of QD-VCSEL with the progressively increased pump intensity. As the pump intensity increased above lasing threshold, the single-mode sharp laser output was clearly detected at ~ 633 nm with a narrower FWHM of ~ 0.9 nm, and thus estimating *Q*-factor of ~ 703 according to the relationship between lasing wavelength (λ) and mode FWHM ($\Delta\lambda$) by the equation $Q = \lambda/\Delta\lambda$, indicating the high quality of the QD-VCSEL device. The lasing threshold for our QD-VCSEL device was determined to be as low as ~ 3.3 μJ cm^{-2}, which was lower than the reported values for thick-shell CdSe/CdS QDs distributed feedback laser (~28 μJ cm^{-2}) and CdSe/CdS quantum dot-in-rods coffee-ring microlaser (~10 μJ cm^{-2}). [34,35] In addition to the enhanced gain performance of thick-shell CdSe/CdS@ZnO QDs by ZnO sol ligands, the superior lasing performance might be associated with the enhanced mode coupling effect inside the high-quality optical microcavity and the high refractive index QDs layer with low propagation loss.[20,43,59] Meanwhile, the lasing dynamics in our device was explored by measuring their time-resolved emission spectrogram (Fig. 7**d**), which exhibited an ultrafast lifetime of ~ 10.5 ps (Fig. 7**e**) and primarily limited by the response time of streak camera system. Furthermore, the measured lasing emission intensity of QD-VCSEL device was robustly stable above 93% of initial intensity under 1.8 × 10^7 shots of femtosecond pulse pump at atmospheric conditions (**Fig. S12**). After operating for continuous 5 h, no apparent spectral variation or shift was observed in the lasing spectra, revealing that the constructed QD-microlaser possesses excellent operation stability for potential commercial application.

3. Conclusion

In summary, we successfully prepared the monodisperse CdSe/CdS@ZnO QDs by a facile strategy that capped with inorganic ZnO sol as surface ligands. Compared to the conventional QDs composite, the as-prepared CdSe/CdS@ZnO QDs retained the natural advantages of solution-processed fabrication and single-particle-level application, and also showing outstanding colloidal stability in solution. Significantly, ZnO sol here acted as both surface ligands and electron acceptor plays important roles for the passivation of surface defects and maintaining neutral state of QDs, thus remarkably enhancing their optical properties and stability. At the same time, as expected that the CdSe/CdS@ZnO QDs film exhibited the improved PL thermal stability, and no obvious spectra shift and broadening under continuous thermal treatment, which was in sharp contrast to the CdSe/CdS QDs film. Moreover, the close-packed CdSe/CdS@ZnO QDs film also performed the superior ASE performance. As a further application-oriented exploration, we finally fabricated a high-quality VCSEL device based on CdSe/CdS@ZnO QDs, which displayed the high-performance single-mode lasing operation and excellent device performance stability. Therefore, these results demonstrate that the presented reconstruction strategy for the inorganic sol ligands of QDs opens up a potential way to prepare all-inorganic semiconductor nanomaterials. More importantly, this work will hopefully overcome the limitations that resulted from the surface organic ligands of colloidal semiconductor nanomaterials for practical optoelectronic

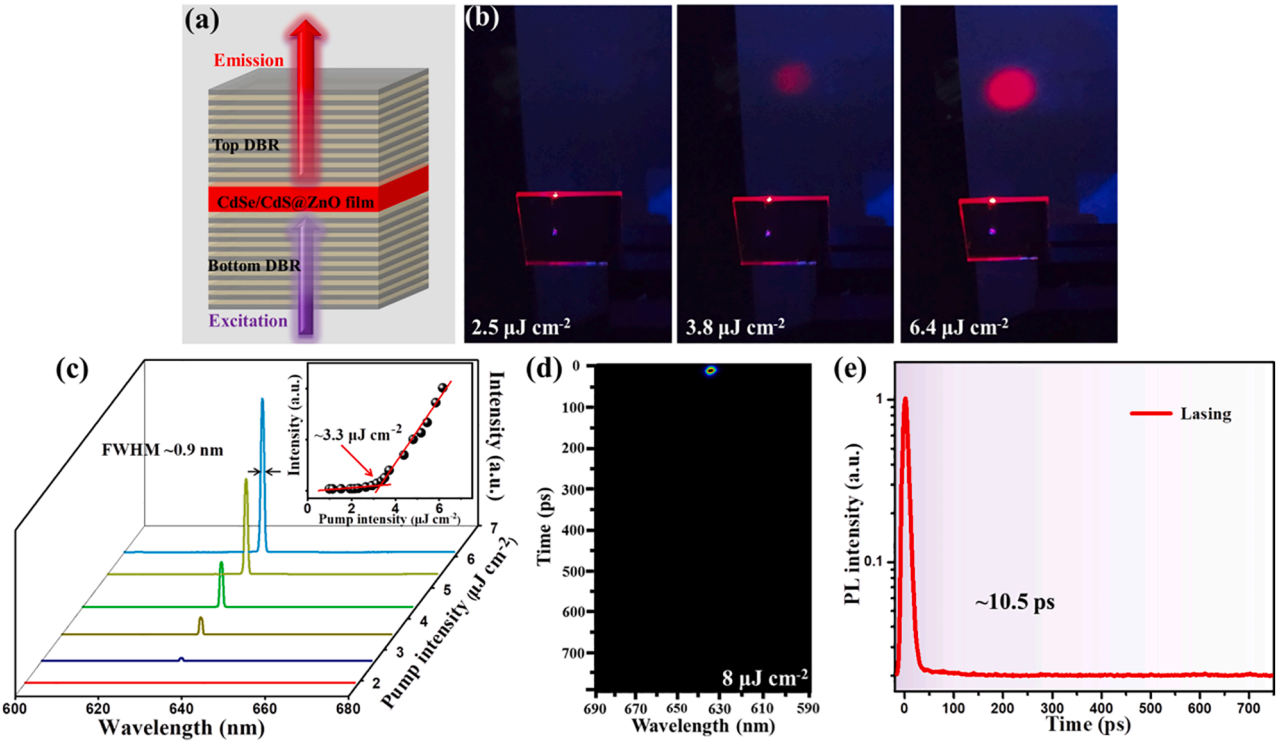

Fig. 7. (a) Schematic configuration of the CdSe/CdS@ZnO QDs vertical cavity surface-emitting lasers. (b) Photograph of thick-shell CdSe/CdS@ZnO QDs laser device in operation under pump intensity of 2.5, 3.8, and 6.4 μJ cm^{-2}, respectively. (c) Pump-dependent emission spectra from the device; the inset shows the emission intensity at the sharp peak versus pump intensity. (d) Time-resolved emission spectrogram of the device above the lasing threshold and their corresponding (e) time response trace.

applications.

4. Experimental section

***Synthesis of CdSe/CdS core/shell QDs*:** The synthesis of CdSe/CdS core/shell QDs followed the typical two steps.[34] First, the CdSe cores were synthesized by the heat-injection method at 240 °C. Then, the CdS shell with the controlled thickness was epitaxially grown on the surface of CdSe cores by the successive ionic layer adsorption and reaction approach.

***Preparation of CdSe/CdS@ZnO QDs*:** First, the as-synthesized CdSe/CdS QDs were further purified by N-butyl ether solution to remove the excess, bound ligands (See Supporting Information). At the same time, the ZnO sol solution was synthesized according to an optimizing approach and used after 24 h (See Supporting Information). Then, the above QDs were dispersed in 20 mL chloroform solution and added 0.58 g EA, which was under stirring for 24 h in the dark environment. As the surface of QDs was modified by EA, the dispersity of QDs in chloroform solution became worse, thus resulting in precipitation. The above supernatant was removed and the precipitation could be washed in chloroform solution. Finally, the ZnO sol solution was added dropwise into the QDs precipitation solution while shaking until the precipitation was disappeared and became a clear and transparent solution (**Fig. S1**).

***Fabrication of CdSe/CdS@ZnO QDs VCSEL devices*:** The twelve pairs of quarter-wavelength-thick SiO_2/TiO_2 layers were as the bottom DBR mirror, which was deposited onto the cleaned quartz substrate. The CdSe/CdS@ZnO QDs gain medium layer was fabricated on the surface of bottom DBR mirror by the spin-coating method and combined with immediate annealing process at high temperature (300 °C) in Argon atmosphere. The high-temperature annealing treatment promotes to crystallize the CdSe/CdS@ZnO QDs film. The solvents, residual EA, and zinc acetate dehydrate could be evaporated thoroughly under such high temperature. Then, the above QDs film was put into the vacuum axe keeping 24 h for further utilization. Finally, the high-reflection (~99%) top DBR mirror (alternating CaF_2/ZnS layers) was deposited on top of QDs layer by electron beam deposition at room temperature. Each alternating layers were controlled to be a quarter of emission wavelength.

***Structural characterizations*:** TEM and HAADF STEM images were obtained on an FEI Tecnai G2 electron microscope. The cross-section image of QD-VCSELs was measured by Carl Zeiss Ultra Plus field emission scanning electron microscopy (SEM). XRD patterns were acquired using an X-ray diffractometer (Bruker, D8-DISCOVER) with *Cu* Kα source. FTIR spectra were measured on a Nicolet iS10 infrared spectrometer.

***Optical measurements*:** The absorption spectra were measured on a UV–vis-NIR spectrophotometer (UV3600, Shimadzu). The PL spectra and time-resolved PL decay traces were recorded using Edinburgh F900 luminescence spectrometer at room temperature, PL decay traces were monitored at the PL peak wavelength for each sample. The PL QY of the samples was measured relative to a standard dye (Rhodamine B (QY, 50%)) at an identical optical density. Biexciton recombination dynamics measurements were performed in QDs solution, a femtosecond Ti: Sapphire laser with a frequency-doubling external β-barium borate crystal (400 nm, 1 kHz, 100 fs; Legend-F-1 k, Coherent) was used as the pump source. The emission signal was collected by an electrically triggered streak camera system (Hamamatsu C5680), and the temporal evolution of the PL spectra was extracted from the center of peak wavelength. For the photostability measurement, the QDs solution was placed under a UV lamp (365 nm, ~75 mW cm^{-2}) and the QDs film was put onto an accurately temperature controlled heating platform (IKA) under heated to 100 °C within inert gas atmosphere, and then PL spectra were recorded by a Shimadzu spectrofluorometer (RF-5301PC) under the excitation wavelength of 400 nm. For the blinking measurement, a picosecond supercontinuum fiber laser (490 nm, 4.9 MHz; NKT Photonics EXR-15) was employed as the excitation source. For ASE measurement, a stripe pump (400 nm, 100 fs) was acquired using a cylindrical lens (10 cm focal length). The stripe modal confined pump pulses were perpendicular to the surface of QDs film, and then the emission from the film edge was collected by the fast optical multichannel analyzer (OMA, SpectraPro-300i, Acton Research Corporation) and optically triggered streak camera system. The intensity of the pump pulse was set as three times of ASE threshold for emission stability measurement. For the lasing measurement, the pump beam (400 nm, 100 fs) was focused by a convex lens (5 cm focus length) onto the VCSEL, and the output signal was collected from the other side of the VCSEL along the normal direction by the OMA and optically triggered streak camera system for steady and transient spectra, respectively.

Declaration of Competing Interest

The authors declare that they have no known competing financial interests or personal relationships that could have appeared to influence the work reported in this paper.

Acknowledgements

This work was supported by the National Natural Science Foundation of China (12004201), the Postgraduate Research & Practice Innovation Program of Jiangsu Province (KYCX17_0064), and the Science and Technology Support Program of Jiangsu Province (BE2018117).

Appendix A. Supplementary data

Supplementary data to this article can be found online at https://doi.org/10.1016/j.cej.2021.131159.

References

[1] S.M. Wichner, V.R. Mann, A.S. Powers, M.A. Segal, M. Mir, J.N. Bandaria, M. A. DeWitt, X. Darzacq, A. Yildiz, B.E. Cohen, Covalent protein labeling and improved single-molecule optical properties of aqueous CdSe/CdS quantum dots, ACS Nano 11 (7) (2017) 6773–6781.
[2] M. Zhao, Q. Zhang, Z. Xia, Narrow-Band Emitters in LED Backlights for Liquid-Crystal Displays, Mater. Today 40 (2020) 246–265.
[3] O.V. Kozlov, Y.-S. Park, J. Roh, I. Fedin, T. Nakotte, V.I. Klimov, Sub–single-exciton lasing using charged quantum dots coupled to a distributed feedback cavity, Science 365 (6454) (2019) 672–675.
[4] Y.-S. Park, S. Guo, N.S. Makarov, V.I. Klimov, Room temperature single-photon emission from individual perovskite quantum dots, ACS Nano 9 (2015) 10386–10393.
[5] J. Zhou, M. Zhu, R. Meng, H. Qin, X. Peng, Ideal CdSe/CdS Core/Shell nanocrystals enabled by entropic ligands and their core size-, shell thickness-, and ligand-dependent photoluminescence properties, J. Am. Chem. Soc. 139 (46) (2017) 16556–16567.
[6] M.Q. Dai, L.Y.L. Yung, Ethylenediamine-assisted ligand exchange and phase transfer of oleophilic quantum dots: stripping of original ligands and preservation of photoluminescence, Chem. Mater. 25 (2013) 2193–2201.
[7] Z. Yang, Q. Wu, G. Lin, X. Zhou, W. Wu, X. Yang, J. Zhang, W. Li, All-solution processed inverted green quantum dot light-emitting diodes with concurrent high efficiency and long lifetime, Mater. Horiz. 6 (2019) 2009–2015.
[8] E. Socie, B.R.C. Vale, A. Burgos-Caminal, J.-E. Moser, Direct observation of shallow trap states in thermal equilibrium with band-edge excitons in strongly confined cspbbr 3 perovskite nanoplatelets, Adv. Opt. Mater. 9 (2021) 2001308.
[9] J.M. Pietryga, Y. Park, J. Lim, A.F. Fidler, W.K. Bae, S. Brovelli, V.I. Klimov, Spectroscopic and device aspects of nanocrystal quantum dots, Chem. Rev. 116 (2016) 10513–10622.
[10] Y. Kuang, C. Zhu, W. He, X. Wang, Y. He, X. Ran, L. Guo, Regulated exciton dynamics and optical properties of single perovskite cspbbr 3 quantum dots by diluting surface ligands, J. Phys. Chem. C 124 (2020) 23905–23912.
[11] S. Ghosh, D. Kushavah, S.K. Pal, Unravelling the role of surface traps on carrier relaxation and transfer dynamics in ultrasmall semiconductor nanocrystals, J. Phys. Chem. C 122 (2018) 21677–21685.
[12] M. Califano, F.M. Gómez-Campos, Universal trapping mechanism in semiconductor nanocrystals, Nano Lett. 13 (5) (2013) 2047–2052.
[13] Y. Shirasaki, G.J. Supran, M.G. Bawendi, V. Bulović, Emergence of colloidal quantum-dot light-emitting technologies, Nat. Photonics 7 (1) (2013) 13–23.
[14] C.D. Pu, X.L. Dai, Y.F. Shu, M.Y. Zhu, Y.Z. Deng, Y.Z. Jin, X.G. Peng, Electrochemically-stable ligands bridge the photoluminescence-electroluminescence gap of quantum dots, Nat. Commun. 11 (2020) 937.

[15] P. Reiss, M. Protiere, L. Li, Core/Shell semiconductor nanocrystals, Small 5 (2009) 154–168.
[16] S.T. Selvan, P.K. Patra, C.Y. Ang, J.Y. Ying, Synthesis of silica-coated semiconductor and magnetic quantum dots and their use in the imaging of live cells, Angew. Chem. Int. Ed. 46 (2007) 2448–2452.
[17] T.-H. Le, Y. Choi, S. Kim, U. Lee, E. Heo, H. Lee, S. Chae, W.B. Im, H. Yoon, Highly elastic and >200% reversibly stretchable down-conversion white light-emitting diodes based on quantum dot gel emitters, Adv. Opt. Mater. 8 (2020) 1901972.
[18] S. Jun, J. Lee, E. Jang, Highly luminescent and photostable quantum dot-silica monolith and its application to light-emitting diodes, ACS Nano 7 (2) (2013) 1472–1477.
[19] C. Sun, Y.u. Zhang, C. Ruan, C. Yin, X. Wang, Y. Wang, W.W. Yu, Efficient and stable white leds with silica-coated inorganic perovskite quantum dots, Adv. Mater. 28 (45) (2016) 10088–10094.
[20] J. Jasieniak, J. Pacifico, R. Signorini, A. Chiasera, M. Ferrari, A. Martucci, P. Mulvaney, Luminescence and amplified stimulated emission in cds-zns-nanocrystal-doped tio$_2$ and zro$_2$ waveguides, Adv. Funct. Mater. 17 (2007) 1654–1662.
[21] Y. Chen, J. Vela, H. Htoon, J.L. Casson, D.J. Werder, D.A. Bussian, V.I. Klimov, J. A. Hollingsworth, "Giant" multishell cdse nanocrystal quantum dots with suppressed blinking, J. Am. Chem. Soc. 130 (2008) 5026–5027.
[22] O. Chen, J. Zhao, V.P. Chauhan, J. Cui, C. Wong, D.K. Harris, H. Wei, H.-S. Han, D. Fukumura, R.K. Jain, M.G. Bawendi, Compact high-quality cdse-cds core-shell nanocrystals with narrow emission linewidths and suppressed blinking, Nat. Mater. 12 (2013) 445–451.
[23] R. Xie, U. Kolb, J. Li, T. Basché, A. Mews, Synthesis and Characterization of Highly Luminescent CdSe-Core CdS/Zn$_{0.5}$Cd$_{0.5}$S/ZnS multishell nanocrystals, J. Am. Chem. Soc. 127 (20) (2005) 7480–7488.
[24] B. Wang, C. Zhang, S. Huang, Z. Li, L. Kong, L. Jin, J. Wang, K. Wu, L. Li, Postsynthesis phase transformation for cspbbr 3/r$_b$4pbb$_r$4 core/shell nanocrystals with exceptional photostability, ACS Appl Mater. Interfaces 10 (2018) 23303–23310.
[25] X.S. Tang, J. Yang, S.Q. Li, Z.Z. Liu, Z.P. Hu, J.Y. Hao, J. Du, Y.X. Leng, H.Y. Qin, X. Lin, Y. Lin, Y.X. Tian, M. Zhou, Q.H. Xiong, Single halide perovskite/semiconductor core/shell quantum dots with ultrastability and nonblinking properties, Adv. Sci. 6 (2019) 1970107.
[26] J. Lim, Y.-S. Park, V.I. Klimov, Optical gain in colloidal quantum dots achieved with direct-current electrical pumping, Nat. Mater. 17 (1) (2018) 42–49.
[27] F. García-Santamaría, Y. Chen, J. Vela, R.D. Schaller, J.A. Hollingsworth, V. I. Klimov, Suppressed auger recombination in "giant" nanocrystals boosts optical gain performance, Nano Lett. 9 (2009) 3482–3488.
[28] C. Galland, Y. Ghosh, A. Steinbrück, M. Sykora, J.A. Hollingsworth, V.I. Klimov, H. Htoon, Two types of luminescence blinking revealed by spectroelectrochemistry of single quantum dots, Nature 479 (7372) (2011) 203–207.
[29] S.O.M. Hinterding, S.J.W. Vonk, E.J. van Harten, F.T. Rabouw, Dynamics of intermittent delayed emission in single cdse/cds quantum dots, J. Phys. Chem. Lett. 11 (12) (2020) 4755–4761.
[30] M. Zhu, J. Zhou, Z. Hu, H. Qin, X. Peng, Effects of local dielectric environment on single-molecule spectroscopy of a cdse/cds core/shell quantum dot, ACS Photonics 5 (10) (2018) 4139–4146.
[31] E.M. Thomas, S. Ghimire, R. Kohara, A.N. Anil, K. Yuyama, Y. Takano, K. G. Thomas, V.P. Biju, Blinking suppression in highly excited cdse/zns quantum dots by electron transfer under large positive gibbs (free) energy change, ACS Nano 12 (2018) 9060–9069.
[32] Z. Hu, S. Liu, H. Qin, J. Zhou, X. Peng, Oxygen stabilizes photoluminescence of cdse/cds core/shell quantum dots via deionization, J. Am. Chem. Soc. 142 (9) (2020) 4254–4264.
[33] V. Naresh, B.H. Kim, N. Lee, Synthesis of $CsPbX_3$ (X = Cl/Br, Br, and Br/I)@SiO_2/PMMA composite films as color-conversion materials for achieving tunable multi-color and white light emission, Nano Res. 14 (2021) 1187–1194.
[34] L. Zhang, C. Liao, B. Lv, X. Wang, M. Xiao, R. Xu, Y. Yuan, C. Lu, Y. Cui, J. Zhang, Single-mode lasing from "giant" cdse/cds core-shell quantum dots in distributed feedback structures, ACS Appl. Mater. Interfaces 9 (2017) 13293–13303.
[35] F. Di Stasio, J.Q. Grim, V. Lesnyak, P. Rastogi, L. Manna, I. Moreels, R. Krahne, Single-mode lasing from colloidal water-soluble cdse/cds quantum dot-in-rods, Small 11 (2015) 1328–1334.
[36] C.H. Lin, E. Lafalce, J. Jung, M.J. Smith, S.T. Malak, S. Aryal, Y.J. Yoon, Y. Zhai, Z. Lin, Z.V. Vardeny, V.V. Tsukruk, Core/Alloyed-shell quantum dot robust solid films with high optical gains, ACS Photonics 3 (4) (2016) 647–658.
[37] Y. Ghosh, B.D. Mangum, J.L. Casson, D.J. Williams, H. Htoon, J.A. Hollingsworth, New insights into the complexities of shell growth and the strong influence of particle volume in nonblinking "giant" core/shell nanocrystal quantum dots, J. Am. Chem. Soc. 134 (2012) 9634–9643.
[38] A. Pakdel, F. Ghodsi, Influence of drying conditions on the optical and structural properties of sol–gel-derived ZnO nanocrystalline films, Pramana 76 (2011) 973–983.
[39] P.H. Vajargah, H. Abdizadeh, R. Ebrahimifard, M.R. Golobostanfard, Sol-gel derived ZnO thin films: effect of amino-additives, Appl. Surf. Sci. 285 (2013) 732–743.
[40] A. Heuer-Jungemann, N. Feliu, I. Bakaimi, M. Hamaly, A. Alkilany, I. Chakraborty, A. Masood, M.F. Casula, A. Kostopoulou, E. Oh, K. Susumu, M.H. Stewart, I. L. Medintz, E. Stratakis, W.J. Parak, A.G. Kanaras, The role of ligands in the chemical synthesis and applications of inorganic nanoparticles, Chem. Rev. 119 (2019) 4819–4880.
[41] A. Prudnikau, D.I. Shiman, E. Ksendzov, J. Harwell, E.A. Bolotina, P.A. Nikishau, S. V. Kostjuk, I.D.W. Samuelc, V. Lesnyak, Design of cross-linked polyisobutylene matrix for efficient encapsulation of quantum dots, Nanoscale Adv. 3 (2021) 1443–1454.
[42] R. Kim, H.S. Park, T. Yu, J. Yi, W.-S. Kim, Aqueous synthesis and stabilization of highly concentrated gold nanoparticles nanoparticles using sterically hindered functional polymer, Chem. Phys. Lett. 575 (2013) 71–75.
[43] M. Caglar, S. Ilican, Y. Caglar, Influence of dopant concentration on the optical properties of zno, Films by Sol-Gel Method, Thin Solid Films 517 (17) (2009) 5023–5028.
[44] X. Wang, L. Qu, J. Zhang, X. Peng, M. Xiao, Surface-related emission in highly luminescent cdse quantum dots, Nano Lett. 3 (8) (2003) 1103–1106.
[45] S.C. Boehme, J.M. Azpiroz, Y.V. Aulin, F.C. Grozema, D. Vanmaekelbergh, L. D. Siebbeles, I. Infante, A.J. Houtepen, Density of trap states and auger-mediated electron trapping in cdte quantum-dot solids, Nano Lett. 15 (2015) 3056–3066.
[46] Y. Cai, Y. Li, L. Wang, R.-J. Xie, A facile synthesis of water-resistant cspbbr 3 perovskite quantum dots loaded poly (methyl methacrylate) composite microspheres based on in situ polymerization, Adv. Opt. Mater. 7 (2019) 1901075.
[47] V.I. Klimov, A.A. Mikhailovsky, D.W. McBranch, C.A. Leatherdale, M.G. Bawendi, Quantization of multiparticle auger rates in semiconductor quantum dots, Science 287 (2000) 1011–1013.
[48] M. Abdellah, K. Žídek, K. Zheng, P. Chábera, M.E. Messing, T. Pullerits, Balancing electron transfer and surface passivation in gradient cdse/zns core-shell quantum dots attached to zno, J. Phys. Chem. Lett. 4 (11) (2013) 1760–1765.
[49] M.G. Bawendi, P.J. Carroll, W.L. Wilson, L.E. Brus, Luminescence properties of cdse quantum crystallites: resonance between interior and surface localized states, J. Chem. Phys. 96 (2) (1992) 946–954.
[50] J.M. Zhang, X.K. Zhang, J.Y. Zhang, Size-dependent time-resolved photoluminescence of colloidal cdse nanocrystals, J. Phys. Chem. C 113 (2009) 9512–9515.
[51] L. Zou, Z. Fang, Z. Gu, X. Zhong, Aqueous phase synthesis of biostabilizer capped cds nanocrystals with bright emission, J. Lumin. 129 (5) (2009) 536–540.
[52] Y. Ma, Y. Li, S. Ma, X. Zhong, Highly bright water-soluble silica coated quantum dots with excellent stability, J. Mater. Chem. B 2 (31) (2014) 5043–5051.
[53] M.M. Krause, J. Mooney, P. Kambhampati, Chemical and thermodynamic control of the surface of semiconductor nanocrystals for designer white light emitters, ACS Nano 7 (7) (2013) 5922–5929.
[54] J. Mooney, M.M. Krause, J.I. Saari, P. Kambhampati, A Microscopic picture of surface charge trapping in semiconductor nanocrystals, J. Chem. Phys. 138 (20) (2013) 204705, https://doi.org/10.1063/1.4807054.
[55] L. Znaidi, Sol-gel-deposited zno thin films: A review, Mater. Sci. Eng., B 174 (1-3) (2010) 18–30.
[56] A.F. Cihan, Y. Kelestemur, B. Guzelturk, O. Yerli, U. Kurum, H.G. Yaglioglu, A. Elmali, H.V. Demir, Attractive versus repulsive excitonic interactions of colloidal quantum dots control blue- to red-shifting (and non-shifting) amplified spontaneous emission, J. Phys. Chem. Lett. 4 (2013) 4146–4152.
[57] D.I. Chepic, A.L. Efros, A.I. Ekimov, M.G. Ivanov, V.A. Kharchenko, I. A. Kudriavtsev, T.V. Yazeva, Auger ionization of semiconductor quantum drops in a glass matrix, J. Lumin. 47 (3) (1990) 113–127.
[58] C. Liao, K. Fan, R. Xu, H. Zhang, C. Lu, Y. Cui, J. Zhang, Laser-annealing-made amplified spontaneous emission of "giant" cdse/cds core/shell nanocrystals transferred from bulk-like shell to quantum-confined core, Photonics Res. 3 (2015) 200–205.
[59] R. Castanedo-Pérez, O. Jiménez-Sandoval, S. Jiménez-Sandoval, J. Márquez-Marín, A. Mendoza-Galván, G. Torres-Delgado, A. Maldonado-Alvarez, Influence of annealing temperature on the formation and characteristics of sol-gel prepared zno films, J. Vac. Sci. Technol., A 17 (4) (1999) 1811–1816.